IRIS AperTO

UNIVERSITÀ DEGLI STUDI DI TORINO

AperTO - Archivio Istituzionale Open Access dell'Università di Torino

Genetic control and evolution of anthocyanin methylation

This is a pre print version of the following article:

Original Citation:

Availability:

This version is available http://hdl.handle.net/2318/1524843 since 2015-09-13T10:57:08Z

Published version:

DOI:10.1104/pp.113.234526

Terms of use:

Open Access

Anyone can freely access the full text of works made available as "Open Access". Works made available under a Creative Commons license can be used according to the terms and conditions of said license. Use of all other works requires consent of the right holder (author or publisher) if not exempted from copyright protection by the applicable law.

(Article begins on next page)

13 December 2025

Genetics and evolution of anthocyanin methylation

Research Area: Biochemistry and Metabolism

Corresponding authors:

Francesca Quattrocchio, Department of Molecular Cell Biology, VU University, de Boelelaan 1085, 1081HV Amsterdam, The Netherlands. Tel: +31-205987202, Email: f.m.quattrocchio@vu.nl

Ronald Koes, Department of Molecular Cell Biology, VU University, de Boelelaan 1085, 1081HV Amsterdam, The Netherlands. Tel: +31-205987201, Email: ronald.koes@vu.nl

Genetic control and evolution of anthocyanin methylation[1][W]

Sofia Provenzano[2], Cornelis Spelt[2], Satoko Hosokawa, Noriko Nakamura, Filippa Brugliera[3], Linda Demelis, Daan P. Geerke, Andrea Schubert, Yoshikazu Tanaka, Francesca Quattrocchio[*] and Ronald Koes[*]

Department of Molecular Cell Biology, Graduate School of Experimental Plant Sciences, VU University, The Netherlands (S.P., C.S., F.Q., R.K.), Research Institute, Suntory Global Innovation Center Ltd, 1-1-1 Wakayamadai, Shimamoto, Mishima, Osaka, Japan (S.H., N.N., Y.T.), Florigene Pty. Ltd., 1 Park Drive, Bundoora, VIC 3083, Australia (F.B., L.D.), AIMMS Division of Molecular Toxicology, VU University, The Netherlands (D.P.G.) and Department of Agricultural and Food Sciences, University of Turin, 10095 Grugliasco, Italy (S.P., A.S.).

One sentence summary: *.Analysis of anthocyanin methyltransferase genes reveals genetic mechanisms underlying the evolution of anthocyanins with diverse structures*.

[1]This work was supported by a COST fellowship (COST-STSM-858-4287) to S.P. Work at the VU was financed by Departmental funds earned with teaching.

[2]These authors contributed equally

[3]Current address: LaTrobe Institute of Molecular Sciences, La Trobe University, Kingsbury Drive, Bundoora, 3086, Victoria, Australia

[*] Address correspondence to ronald.koes@vu.nl, or f.m.quattrocchio@vu.nl

ABSTRACT

Anthocyanins are a chemically diverse class of secondary metabolites that color most flowers and fruits. They consist of three aromatic rings that can be substituted with hydroxyl, sugar, acyl and methyl groups in a variety of patterns depending on the plant species. To understand how such chemical diversity evolved we isolated and characterized *METHYLATION AT THREE2* (*MT2*) and the two *METHYLATION AT FIVE* (*MF*) loci from petunia, which direct anthocyanin methylation in petals. The proteins encoded by *MT2* and the duplicated *MF1* and *MF2* genes, and a putative grape homolog VvAOMT1 are highly similar to and apparently evolved from caffeoylCoA *O*-methyltransferases by relatively small alterations in the active site. Transgenic experiments showed that the petunia and grape enzymes have remarkably different substrate specificities, which explains part of the structural anthocyanin diversity in both species. Most strikingly, VvAOMT1 expression resulted in the accumulation of novel anthocyanins that are normally not found in petunia, revealing how alterations in the last reaction can reshuffle the pathway and affect (normally) preceding decoration steps in an unanticipated way. Our data show how variations in gene expression patterns, loss-of function mutations, and alterations in substrate specificities all contributed to the anthocyanins' structural diversity.

INTRODUCTION

Distinct plant species produce presumably hundreds of thousands of secondary metabolites, which are low molecular weight compounds that occur in some specific groups only (Pichersky and Gang, 2000). Flavonoids, for example, are a major family of secondary metabolites found in virtually all vascular plants, that are involved in protection against UV-light and pathogens, signaling to nodulating bacteria, hormone transport, pollen germination and the coloration of flowers and fruits. This functional diversity is paralleled by a large chemical diversity as today over 9000 flavonoids with distinct structures have been identified in variety of species (Buer et al., 2010). How the ability to synthesize such a vast number of different compounds has evolved is largely unknown, but presumably involved gene duplications and divergence of encoded proteins and gene expression patterns (Pichersky and Gang, 2000).

Flavonoid biosynthesis is arguably one of the best-studied pathways in plants, in particular the early steps that generate the flavonoid "scaffolds" of various subclasses, like flavanols and anthocyanins. However, much less is known about the subsequent modifications ("decorations"), such as glycosylation, acylation and methylation, which cause most of the structural variation (Grotewold, 2006). Grape (*Vitis vinifera*), for example, synthesizes very simple anthocyanins bearing one or two methyl groups and a single (acetylated) sugar, whereas *Arabidopsis* accumulates more complex anthocyanins with seven sugar and acyl moieties but no methyl groups (Brouillard et al., 2003; Saito et al., 2013), and *Petunia* pigments its petals with methylated anthocyanins that bear an acylated rutinoside moiety (Ando et al., 1999; Slimestad et al., 1999).

Petunia hybrida (garden petunia) was generated 200 years ago by interspecific crosses between various accessions/subspecies of *P. inflata* and *P. axillaris*. *P. inflata* subspecies have bee-pollinated flowers with violet petals containing 3'5'-methylated anthocyanins (malvidins), while *P. axillaris* accessions have moth–pollinated flowers with a white corolla limb that lacks anthocyanins, and a variegated corolla tube containing anthocyanins that lack one or both methyl groups (Quattrocchio et al., 1999; Hoballah et al., 2007). Classical breeding generated *P. hybrida* cultivars, each containing a different "mix" of the parental species genomes, with a wide variety of flower colors resulting from the introgression of mutant alleles from the parental species (Quattrocchio et al., 1999) and new mutations that arose in *P. hybrida* (Kroon et al., 1994; van Houwelingen et al., 1998).

Analysis of segregating populations of unrelated *P. hybrida* cultivars identified several loci controlling the decoration of anthocyanins and suggested a model for their sequential action (Wiering, 1974; Wiering and De Vlaming, 1977; de Vlaming et al., 1984). This model (Figure 1A) was substantiated by enzymological analyses in the 1980s (Jonsson et al., 1982; Jonsson et al., 1983; Jonsson et al., 1984; Jonsson et al., 1984) and, more recently, the isolation of some of the genes (Brugliera et al., 1993; Kroon et al., 1994; Yamazaki et al., 2002). The current view is that anthocyanin-3 glucosides are in the petal limb sequentially

(*i*) rhamnosylated by a sugar-transferase encoded by *RHAMNOSYLATION AT THREE* (*RT*) (Br[illegible]ra et al., 1993; Kroon et al., 1994), (*ii*) acylated by an anthocyanin acyltransferase (AAT) encoded by *GLUCOSYLATION AT FIVE* (*GF)* (Provenzano, 2011), (*iii*) 5-glucosylated by a 5-glucosyltransferase (5GT) (Yamazaki et al., 200[illegible]d (*iv*) methylated in the 5' and/or 3' position by anthocyanin methyltransferases (AMTs) (Figure 1A).

Genetic analyses suggested that three or four partially redundant loci control the methylation of anthocyanins in petunia petals (Wiering, 1974; Wiering and De Vlaming, 1977) and the activity/expression multiple AMT isoforms with different isoelectric points (Jonsson et al., 1983; [illegible]on et al., 1984). *METHYLATION AT THREE* (*MT*) directs methylation of the 3' hydroxyl group and *METHYLATION AT FIVE* (*MF*) directs methylation of both the 3' and 5' hydroxyl group. Segregation ratios of 3'5' methylation in certain crosses and linkage to markers on chromosomes III and V, suggested that two *MF* loci (*MF1* and *MF2*) might exist (Wiering and De Vlaming, 1977), but could also be explained by the translocation of a single *MF* gene in some lines. Because it was originally thought that 3' methylation by an *MT* gene is essential for subsequent 5' methylation by *MF1/2* (Wiering, 1974), two *MT* loci were postulated: one, *MT1,* tightly linked with *MF1* on chromosome III, and another, *MT2,* linked with *MF2* on chromosome V (Wiering, 1974; Wiering a[illegible] Vlaming, 1977). However, analyses of a partially purifie[illegible]Ts from petals (Jonsson et al., 1984) and transgenic experiments with MF2 (this paper) demonstrated that a single enzyme[illegible]5'MT) could methylate both the 3' and 5' position, proving the premise for postulating *MT1* incorrect. Moreover, molecular data, presented here, also indicate that *MT* and *MF* genes constitute a family of only three genes. Hence, we consider the *MT1* locus for this paper as non-existent.

ANTHOCYANIN1 (AN1), AN2 and AN11 are HLH, MYB and WD40 proteins that activate transcription of genes involved in anthocyanin synthesis and vacuolar acidification (Koes et al., 2005). A differential hybridization screen identified cDNAs from seven so-called *DIF* genes that were down-regulated in *an1* petals (Kroon et al., 1994). *DIFa*, *DIFf*, *DIFg* and *DIFi* encode respectively anthocyanidin synthase (ANS), a cytochrome b5 required for hydroxylation by flavonoid 3',5' hydroxylase (F3'5'H) (de Vetten et al., 1999), a sugar-transferase encoded by *RT* (Kroon et al., 1994), and a glutathione-transferase encoded by *AN9* (Alfenito et al., 1998). To iden[illegible]dditional enzymes involved in the decoration of anthocyanins, we analyzed the remaining *DIF* genes. Recent data show that *DIFi* originates from the *GLYCOSYLATION AT FIVE* (*GF*) locus and encodes an acyl-transferase (Provenzano, 2011; manuscript in preparation), while *DIFe1* encodes an AMT (this paper).

Here we show that *DIFe1* and two paralogous genes, *DIFe2a* and *DIFe2b*, encode *O*-methyltransferases that are expressed in petals under the control of AN1, AN2 and AN11 and are located at the *MT2*, *MF1* and *MF2* locus respectively. Complementation experiments with *mt2 mf1 mf2* mutants in distinct genetic backgrounds revealed remarkable differences in the substrate specificities of these petunia AMTs and a putative anthocyanin *O*-methyltransferase from grape (VvAOMT1; Hugueney et al., 2009). Our data provide insight into the molecular genetic mechanisms underlying the evolution of distinct anthocyanin structures.

RESULTS

Identification of a putative anthocyanin methyltransferase gene from *Petunia hybrida*

RNA gel-blot analysis showed that expression of mRNAs hybridizing to *DIFe1* is downregulated in lines with mutations in all *MT* and *MF* genes (Figure 1B). Hence, we examined whether a His-tagged DIFe1 protein expressed in *E.coli* can methylate delphinidin 3-glucoside (D3G) or delphinidin 3-rutinoside (D3R) *in vitro*, using as a methyl-donor ^{14}C-*S*-adenosyl methionine (SAM). Homogenates from DIFe1-expressing cells converted D3R and D3G into petunidin and malvidin derivatives, as judged by Thin Layer Chromatography. No activity was seen with homogenates from untransformed cells or when SAM was omitted (Supplemental Table 1). In further experiments we analyzed reaction products by HPLC (Figure 2A). In these assays DIFe1 converted D3R, D3G and D3,5G (delphinidin 3, 5-diglucoside) with similar efficiency. In all cases the major products were petunidin derivatives, while malvidin derivatives constituted a smaller but substantial fraction. The D3R and D3G substrates contained low amounts of cyanidin derivatives as impurities, which were converted by DIFe1 into peonidin. These data suggest that DIFe1 has strong A3'MT activity and a low A3'5'MT activity.

To examine *DIFe1* function *in vivo*, we expressed antisense *DIFe1* RNA from a transgene (*MAC:asDIFe1*) driven by the *MAC* promoter (Comai et al., 1990) in *P. hybrida* F1 hybrid V23xR51 (VR). VR is dominant for all known anthocyanin and flavonol genes and has violet petals. One of five *MAC:asDIFe1* transformants (#A) produced petals with a dull reddish color (Figure 2B). In VR flowers 80% of the anthocyanins are malvidin derivatives, whereas the main anthocyanins in the dull reddish *Mac:asDIFe1* petals were delphinidin derivatives, showing that DIFe1 is involved in anthocyanin methylation *in vivo* (Figure 2C).

DIFe1 is part of a small gene family

Screening a petal cDNA library from *P. hybrida* Old Glory Blue (OGB) with *DIFe1* yielded two clones. One (E20) was identical to the original *DIFe1* cDNA from V26, except that its 5' untranslated region (5'UTR) was 25 nucleotides (nt) longer and the 3'UTR region 96 nt shorter. The latter might result from promiscuous priming of oligo-dT on an A-rich region in the 3'UTR during cDNA synthesis or polyadenylation of the mRNA at distinct sites. The coding sequence of the second cDNA (E33) shared 82% nucleotide identity with *DIFe1,* but was disrupted by a 2-bp deletion, indicating that it originated from a paralogous gene, named *DIFe2*, and that OGB contains a mutant allele (*dife2*^{OGB}).

To study the role of *DIFe2 in vivo*, we generated transgenic VR plants containing a *MAC:asDIFe2* transgene that expresses the antisense RNA. One of five *MAC:asDIFe2* transformants displayed a flower color phenotype similar to that of *MAC:asDIFe1,* that was also associated with a strong reduction of anthocyanin methylation (Figure 2C). The high similarity of the *DIFe1* and *DIFe2* sequences and their RNAi

phenotypes, together with the analysis of mutant alleles of these genes (see below), suggests that RNAi silenced both genes (and even a third gene, see below) simultaneously.

We assessed the number of *DIFe* paralogs in the lines V30 (*MT2 mf1 mf2*), R78 (*mt2 mf1 mf2*) and M1 (*MT2 MF1 MF2*) by DNA gel-blot analysis (Figure 3). The *DIFe2* cDNA probe detected three EcoRI fragments and at least two BamHI fragments in each line using low-stringency washing conditions. One of these EcoRI fragments was presumed to contain *DIFe1*, because it was eliminated after high stringency washing and matched exactly in size a fragment hybridizing to *DIFe1* under stringent conditions. The *DIFe2* alleles of lines V30 and M1 lack EcoRI sites(see below), indicating the two other EcoRI fragments detected by *DIFe2* probe under high stringency conditions contain two distinct genes that are both highly similar to *DIFe2*.

When we amplified DNA from the *P. hybrida* lines V30 and M1 or the parental species *P. inflata* S6, we found that most primers complementary to the $DIFe2^{OGB}$ cDNA amplified two distinct genes with exon sequences that are nearly identical, except for a few single nucleotide polymorphisms (SNPs). Because this low number of SNPs is similar to that observed between alleles from different *P. hybrida* accessions, we could not distinguish which of these two genes is allelic to the $DIFe2^{OGB}$ cDNA and therefore designated them *DIFe2a* and *DIFe2b*. *DIFe2a* and *DIFe2b* are not alleles of one locus but paralogs, because we could amplify both genes from a variety of lines that were inbred for > 30 generations.

DIFe genes encode proteins with similarity to *O*-methyltransferases

Plant *O*-methyltransferases constitute a large family made up of two major clades, A and B, consisting of 2 and 3 subgroups respectively (Lam et al., 2007). The DIFe proteins belong to the A1 subfamily (Supplemental Figure 1, Supplemental Table 2), which contains Caffeoyl-CoA *O*-methyltransferases (CCoA-MTs), and an AMT from grape known as VvAOMT1 (Hugueney et al., 2009), also known as flavanol and anthocyanin O-methyltransferase (FAOMT, Lucker et al., 2011). Other (putative) flavonoid methyltransferases, such as the *Arabidopsis* flavanol 3'methylase AtOMT1 (Saito et al., 2013), and enzymes with similar activities from *Catharanthus* and *Mentha*, belong to the B1 and B2 groups (Lam et al., 2007; Supplemental Figure 1), and are only distantly related to DIFe proteins.

A more detailed analysis, focused on proteins of the A1 subfamily (Figures 4 and Supplemental Table 3), shows that DIFe proteins are very similar and probably orthologous to three grape paralogs, including VvAOMT1, and closely related (predicted) proteins in other Asterids (e.g. *Solanum lycopersicum* and *S. tuberosum*) and Rosids (e.g. *Fragaria vesca* and *Prunus persica*), the major clades in eudicots. The relationship between these proteins resembles that of the species, consistent with the idea that they are orthologous. Interestingly, the two most similar proteins from the Rosid *Arabidopsis* (At1g67980 and At1g67990) fall just outside the DIFe/VvAOMT1 clade, and the next most similar protein (At4g26220) belongs to a phylogenetically distinct subclass of proteins that includes homologous enzymes from *Mesembryantum* (PFOMT) and *Stellaria* that have broad substrate specificity and can methylate flavanols

and caffeic acid esters *in vitro* (Ibdah et al., 2003) and related proteins from cyclamen (Akita et al., 2011). This suggests that *Arabidopsis*, which does not methylate anthocyanins (Saito et al., 2013), lacks a true DIFe/VvAOMT1 homolog. We found no clear DIFe/VvAOMT1 homologs in monocot species either; the most similar proteins from maize (*Zea mays*) and rice (*Oryza sativa*) fall in the CCoA-MT clade. This suggests that these species, and possibly all monocots, lack true DIFe/VvAOMT1 homolog(s).

Expression patterns of *DIFe* genes.

RNA analyses revealed that *DIFe2a* and *DIFe2b* are primarily expressed in petals and ovaries, but not, or much less, in anthers, sepals, leaves, stems and roots (Figure 5A). The expression of both mRNAs is several-fold higher in the petal limb than in the tube, and peaks in developing flower buds (stage 1-4) and rapidly declines after opening of the flower (Figure 5A), similar to other anthocyanin genes such as *DFR* and *CHS* (Quattrocchio et al., 1993). Although ovaries do not accumulate anthocyanins, they do express structural and regulatory anthocyanin genes for reasons that are unknown (Huits et al., 1994; Spelt et al., 2000). *DIFe1* mRNAs are also abundant in petals. However, *DIFe1* is expressed in the petal limb and tube at a similar level at an almost constant level from developing buds (stage 1-2) to open flowers (stage 6) Furthermore, *DIFe1* displays, in contrast to *DIFe2a* and *DIFe2* a low background expression in a wide range of other tissues.

The WD40, HLH and MYB factors encoded by AN11, AN1 and AN2 respectively activate a range of structural anthocyanin genes (Koes et al., 2005) and also *DIFe* genes (Figure 5B). The *DIFe1* genes are expressed in petals of the line R27, while in isogenic *an1* and *an11* petals their expression is strongly down-regulated, similar to the *DIHYDROFLAVANOL REDUCTASE* (*DFR*). Since no *an2* mutants are available in the R27 background, we used a mutant line (W242) harboring an unstable *an2* allele with a transposon insertion and a derived germinal revertant ($AN2^{REV}$) and found that in this isogenic background the *an2* mutation also reduced *DIFe* expression, to a similar extent as *DFR*.

In summary these data show that both *DIFe* genes are co-expressed in time and place and co-regulated by the AN1-AN2-AN11 complex with other anthocyanin genes like *DFR*.

Analysis of mutant *DIFe* alleles

To determine whether *DIFe1*, *DIFe2a* and *DIFe2b* are encoded or regulated by the *MT* or *MF* loci, we analyzed their expression in stage 3-4 petal limbs of different *P. hybrida* genotypes (Figure 6A). In general expression of *DIFe* genes seemed reduced in *mt, mf1* or *mf2* mutants, but it was difficult to link the observed variation in *DIFe* gene expression to *mt2*, *mf1* and/or *mf2* mutations with certainty, in part because of the divergent genetic backgrounds of the lines used. *DIFe1* mRNA expression is strongly reduced in all accessions containing a mutant *mt2* allele, but is hardly or not at all affected by *mf1* and/or *mf2* mutations. In V30 (*mf1 mf2*) expression of *DIFe2a* was reduced, suggesting that *DIFe2a* may be encoded/regulated by *MF1* or *MF2*. In V23 petals all three *DIFe* genes seem normally expressed, and expression of *DIFe2b* seems

even somewhat enhanced, indicating that the *mf2*^{V32} mutation does not eliminate/reduce the mRNA levels of any of the *DIFe* genes.

To determine whether the *DIFe* genes are located at *MT2* or the *MF* loci we analyzed *DIFe1, DIFe2a* and *DIFe2b* alleles in mutant *P. hybrida* lines and inbred accessions of the two parental species, *P. inflata* and *P. axillaris*. The *DIFe1* alleles of the *P. hybrida mt2 mf1 mf2*, lines R78, V32 and M29 all contain a ~2.4 kb insertion in intron 5, compared to *DIFe1* from M1 (*MT2, MF1, MF2*), V30 (*MT2, mf1, mf2*) or *P. inflata* line S6 (Figure 6B, Supplemental Figure 2). This insertion can account for the reduced *DIFe1* mRNA levels in R78 petals (Figure 6A) and consists of a tandem repeat of a novel 1210-bp transposon-like element, designated *dTPH11,* with 125-bp imperfect terminal inverted repeats (TIRs) having 9 mismatches and is flanked by a 9-bp target site duplication. The *P. axillaris* lines S1 and S26, which accumulate delphinidins in their petal tubes and lack active *MT* and *MF* alleles, also contain this double *dTPH11* insertion. The *P. axillaris* line S2, however, accumulates (3' methylated) petunidins in the petal tube and contains an active *MT2* allele (Jonsson et al., 1984). The *DIFe1*^{S2} allele is identical to that of S6 and M1, except for a few SNPs, and lacks the 2.4 kb insertion or any other obvious lesions, such as nonsense, frameshift or splice site mutations, indicating that *DIFe1*^{S2} is a functional allele (Supplemental Figure 2). Taken together this shows that *DIFe1* resides at the *MT2* locus, and that the mutant *mt2*/*dife1* allele arose under natural conditions in *P. axillaris* and was subsequently introgressed in *P. hybrida*.

The *DIFe2a* and *DIF2b* genes of *P. hybrida* M1 (*MT2*, *MF1*, *MF2*) and *P. inflata* S6 have the same intron-exon architecture as *DIFe1,* though the introns differ in size and sequence (Figure 6C, Suppmemental Figures 3 and 4). *P. hybrida* R78 (*mt2 mf1 mf2*) has a 76-bp deletion at the exon3-intron3 junction of *DIFe2a*, which can explain the reduced *DIFe2a* mRNA expression, and a 13-bp deletion in exon 5 of *DIFe2b* (Figure 6C, Supplemental Figure 3). Line V30 (*MT2 mf1, mf2*) contains the same 13-bp deletion in *DIFe2b*, and multiple insertions and deletion in the coding sequence *DIFe2a*. This indicates that the two *DIFe2* genes do not reside at the *MT2* locus, but at *MF1* and *MF2*. In *P. hybrida* R100 (*MT2 mf1 MF2*) *DIFe2a* is disrupted by the same 76-bp deletion as in line R78, whereas its *DIFe2b* allele seemed functional, as it lacks clear lesions such as frameshift, nonsense or splice site mutations. In *P. hybrida* V23 (*MT MF1 mf2*) *DIFe2b* is disrupted by a 2-bp deletion in exon 4, the same as found in the *DIF2e*^{OGB} cDNA, while the *DIFe2a*^{V23} allele seemed functional. This suggests *DIFe2a* and *DIFe2b* are located at the *MF1* and *MF2* locus respectively.

The *mf1* alleles of *P. axillaris* S1, S2 and S26 all share a 22-bp deletion in exon 4, the same as in *dife2a*^{V30}, and a ~7 kb insertion in exon 2 with features of a retrotransposon, such as ~130 bp terminal direct repeats, and fragments of a putative *GAG/POL* gene. Presumably one or both these mutations inactivated *MF1* in *P. axillaris* early on, whereas the many other deletions and small insertions that are specific for each *P. axillaris* line presumably occurred later, after the gene was inactivated. The *mf2* allele of *P. axillaris* S1, S2 and S26 contained two deletions, of 2 and 13 bp, which are identical to the 2-bp and 13-bp deletions found in the distinct *P. hybrida mf2* alleles (Figure 6C, Supplemental Figure 4). This suggests that *mf2*

alleles arose under natural conditions in *P. axillaris* and were introgressed in *P. hybrida*, although it remains unclear how two distinct deletions in a single *P. axillaris* allele ended up in two separate *P. hybrida* alleles.

Complementation of *Petunia hybrida mt* and *mf* mutants.

Since the wild type progenitors of *mt* and *mf* mutants are not available, their genetic and biochemical characterization relied on comparison with *MT* or *MF* lines in unrelated genetic *P. hybrida* backgrounds (Wiering and De Vlaming, 1977; Jonsson et al., 1983; Jonsson et al., 1984), which can be as different as that of distinct *Petunia* species. To ascertain that the *mt2 mf1 mf2* phenotype is due to the mutations in *DIFe* genes, and to compare mutants with isogenic "wild-types", we expressed MT2, MF2 and VvAOMT1 from the constitutive *35S* promoter in two distinct *mt2 mf1 mf2* backgrounds.

The inbred line R78 (*mt2 mf1 mf2*) has additional mutations that block 5' hydroxylation (*hf1 hf2*) and 5-glycosylation and acylation (*gf*) resulting in a red flower color (Figure 7A; Supplemental Table 4). HPLC of the anthocyanidins showed that most anthocyanins in R78 petals are cyanidin derivatives (~94%), while peonidin, delphinidin, petunidin and malvidin derivatives were found in small amounts only (< 2.5% each) (Figure 7B and Supplemental Figure 5). Both cyanidin and peonidin accumulated as a single anthocyanin species that produced ions with mass to charge ratios (*m/z*) of 595.2 and 609.2 respectively in MS(+) analysis, and ion fragments with *m/z* values corresponding to loss of a rhamnose or a rutinoside moiety, indicating that they are cyanidin and peonidin 3-rutinosides, respectively (Figure 7C and Supplemental Figure 6).

Five of eight *35S:MT2*, ten of twelve *35S:MF2* transformants expressed the transgene and produced similar amounts of mRNA (Figure 7D). Expression of MT2 or MF2 increased the level of peonidins only modestly from ~1% to 6.4±1% and 12.5±3.5 % of the total amount of anthocyanidins, (Figure 7B). LC-MS/MS showed that the peonidins in these *35S:MT2* and *35S:MF2* petals were 3-rutinosides (Figure 7C and Supplemental Figures 5 and 6). AMT enzymes in crude petal extracts from different *P. hybrida* lines could methylate anthocyanins with acylated 3-rutinoside and 5-glucose moieties at 60 μM concentration (K_ms in 2-20 μM range, depending on the genotype used), but no conversion of 3-glucosides or 3-rutinosides was seen at all at a 60 μM concentration, and only relatively little at 1mM concentration suggesting K_ms for these substrates in the mM range (Jonsson et al., 1982; Jonsson et al., 1984). This suggested that MT2 and MF1 methylated only a small fraction of the cyanidin 3-rutinosides in the R78 background because they have a too low affinity/efficiency for these substrates. To test this hypothesis, we expressed in R78 the homologous grape protein VvAOMT1, which can efficiently methylate anthocyanin 3-glucosides and 3-rutinosides *in vitro* with K_ms in the ~7-40 μM range, depending on the conditions used (Hugueney et al., 2009; Lucker et al., 2011). Four of the seven *35S:VvAOMT1* R78 transformants expressed the transgene at roughly similar levels as *35S:MT2* and *35S:MF2* (Figure 7D), which caused a very modest change in petal color, which was only evident in side-by-side comparisons with control flower and difficult to capture by photography (Figure 7A), and increased the amount of peonidins from 1% to about 70% of the total anthocyanins (Figure 7B).

These peonidins accumulated as 3-rutinosides (Figure 7D and Supplemental Figure 6). These data show that VvAOMT1 can efficiently methylate cyanidin 3-rutinoside and/or the cyanidin 3-glucoside precursor *in vivo*, whereas MT2 and MF2 do so with low efficiency/kinetics only.

Next, we introduced the same transgenes into an F1 hybrid (R78 xV32) that is *mt2 mf1 mf2,* but harbors dominant alleles of *HF1*, *HF2* and *GF* resulting in a purple flower color (Figure 7A, Supplemental Table 4). The major anthocyanins in R78xV32 petals are delphinidins, occurring in at least three different molecular species (Figure 7B, Supplemental Figure 5). The most abundant species (peak 1, P1) produced an MS(+) ion with *m/z* 919.2 and fragments with *m/z* 465.1 (delphinidin 5-glucoside) and 303.0 (delphinidin), suggesting it to be a delphinidin 3-(p-coumaroyl)-rutinoside 5-glucoside (Figure 7B and Supplemental Figure 5). Peak 2 has the same *m/z* ratio but a slightly longer retention time and is most likely a stereo-isomer with a sugar and/or coumaroyl group in a different position. The MS/MS(+) spectrum of peak 3, a less abundant anthocyanin, was consistent with delphinidin 3-(caffeoyl)-rutinoside 5-glucoside (Supplemental Figure 5F).

Thirteen of twenty *35S:MT2*, five of six *35S:MF2*, and three of six *35S:VvAOMT1* transformants in the R78xV32 background expressed the transgene to similar levels as the R78 transformants (Figure 7D), which resulted in a slightly more reddish petal color (Figure 7A). HPLC showed that in R78xV32 petals expressing *35S:MT2* most delphinidins are converted into (3' methylated) petunidins and a small amount of (3'5' methylated) malvidins, indicating that MT2 has strong A3'MT activity and a slight A3'5'MT activity (Figure 7B). *35S:MF2* also converted delphinidins into petunidins and malvidins, but the malvidin/petunidin ratio was much higher than in *35S:MT2*, suggesting that MF2 has a stronger A3'5'MT activity than MT2. Although VvAOMT1 expression resulted in methylation of only some 50% of the delphinidins, the ratio of malvidin/petunidin products was even higher than in *35S:MF2* petals, indicating that VvOMT1 has *in vivo* both A3'MT and A3'5'MT activity.

LC-MS/MS showed that expression of MT2 or MF2 in R78xV32 petals yielded several new anthocyanins (peaks 4-7; Figure 7E). Peak 4 produced an ion ([M+]) with *m/z* 933.3 and fragments with *m/z* 771.2, 479.1 and 317.1, consistent with petunidin (p-coumaroyl) rutinoside-5-glucoside (Figure 7E and Supplemental Figures 8 and 9). This structure is supported by an additional fragment with *m/z* 623.1 in MS(-) spectra, originating from the loss of a glucose and coumaroyl group (Supplemental Figure 10). Peak 5 also has *m/z* 933.3 in MS(+), suggesting that it is a positional isomer. Peaks 6 and 7 were identified in a similar way as positional isomers of malvidin 3-(p-coumaroyl)rutinoside 5-glucoside (Figure 7E and Supplemental Figures 8 and 9).

Expression of VvAOMT1 in R78xV32 petals yielded two isoforms of petunidin 3-(p-coumaroyl)rutinoside 5-glucoside (peaks 4 and 5), similar to MT2 and MF2 expression. Surprisingly, the produced malvidins were not malvidin 3-(p-coumaroyl)rutinoside 5-glucoside (peak 6), as in *35S:MF2*, but malvidin 3-glucoside and malvidin 3-rutinoside (peaks 8/9) (Figure 7E, Supplemental Figure 11), which are not normally found in petunia species or mutants. This shows again that VvAOMT1 can, unlike MT2 and

MF2, methylate 3-rutinosides and/or 3-glucosides and reveals, unexpectedly, that precocious 3'5' methylation of rutinosides blocks the acylation and 5-glucosylation by the endogenous petunia enzymes.

Functional divergence of methyltransferases.

Analysis of plant methyl-transferases belonging to other clades than CCoA-MTs and AMTs suggested that their substrate specificities are determined by few amino acids (Wang and Pichersky, 1999; Zubieta et al., 2001; Zubieta et al., 2003). The petunia and grape AMTs and CCoAOMTs share high similarity throughout the protein suggesting that their divergent substrate-specificities also result from relatively small structural differences (Figure 8A). Most residues of *Ms* CCoA-MT from *Medicago sativa* that are involved in binding the SAM and caffeoyl-CoA substrates or dimerization (Ferrer et al., 2005), are conserved in the AMTs (Figure 8A). This suggests that AMTs form, like *Ms* CCoA-MT, dimers with a catalytic site in each monomer, which is consistent with the size of AMT activities observed in crude petal extracts (~ 50kD) (Jonsson et al., 1984). Residues 200-215 in *Ms* CCoA-MT form one side of the pocket that holds the caffeoyl group and are conserved among CCoAMTs (Ferrer et al., 2005), but not in MT2, MF1, MF2 and VvAOMT1 (Figure 8A). Residues 50-64 constitute a second region where CCoMTs diverged from the AMTs.

To study effects of these alterations on substrate binding we used the crystal structure of *Ms* CCoA-MT (PDB structure 1SUI; Ferrer et al., 2005) and Molecular Operator Environment software (MOE version 2011; Chemical Computing Group, Montreal, Canada) to superpose the tri-hydroxylated C-ring of anthocyanin onto the methylated ring of the sinnapoyl-CoA product bound to *Ms* CCoA-MT (Supplemental Figures 12A-B). This position of the C-ring forces the 3-glucose or 3-rutinoside chains to orientate towards Tyr208; other binding conformations lead to steric clashes with (one of the) bulky residues at positions 190, 193 and 238 (Supplemental Figure 12B-C), which are conserved in the AMTs (Figure 8A). In case of a delphinidin 3-(coumaroyl)rutinoside substrate without a 5-glucose group, the 3-(coumaroyl)rutinoside moiety can adopt an orientation as depicted in Supplemental Figures 12D-E. However, our computational analysis suggests that the 5-glucose moiety of the MT and MF substrate is orientated as depicted in Supplemental Figure 12F, to avoid steric hindrance with N-terminal residues of the enzyme (e.g. Lys21). This would in turn result in intrusion of the 5-glucose moiety into the 3-(coumaroyl) rutinoside chain (Supplemental Figures 12F), which offers a possible explanation for the observed replacement of large bulky active-site residues such as Tyr208 and Tyr212 by smaller glycine or leucine residues, to enable occupancy by the 3-(coumaroyl)rutinoside group of the corresponding pocket within the active site (Figures 8B-C). Upon the Tyr208Gly conversion in the petunia AMTs, it may even be possible for the substrate to adopt a conformation as shown in Figures 8D-E. This would require replacement of His56, Trp58, and Asn118 by smaller residues, which is indeed observed in MT2, MF1 and MF2 (Figure 8A).

DISCUSSION

The pathway, enzymes and genes involved in the synthesis of simple anthocyanin 3-glucosides is widely conserved and has been studied in great detail in a variety of species. The subsequent decorations with additional sugar, acyl and methyl groups, which account for most of the structural variation of anthocyanin from different species species has remained largely obscure. The identification of AMTs genes and mutants described here provides shows show alterations in the expression or substrate specificties of decorating enzymes lead to chemical anthocyanin diversity

Genetic control of AMT activities in petunia flowers

Using mutants we show that the three *DIFe* genes indetifeid here are essential for methylation of anthocyanins in Petunia and are located the *MT2, MF1* and *MF2* loci. The finding that *mf1* and *mf2* mutants have lesions in two distinct genes (*DIFe2a* and *DIFe2b*) proves unequivocally that *MF1* and *MF2* are closely related paralogs that presumably arose by a recent gene duplication (shortly) before the separation of the *P. axillaris* and *P. inflata* lineages. *DIFe1* is located at *MT2*, as all *P. hybrida* accessions lacking active *MT* gene(s) contain a non-functional *dife1* allele and 3'-methylation can be restored by *35S:DIFe1*. The existence of a second *MT* gene (*MT1*) that should be tightly linked with *MF1* was postulated because 3' methylation was thought to be an essential prerequisite for subsequent 5' methylation by an *MF* gene. Given that MF1 and MF2 can produce both 3' and 3'5' methylated anthocyanins, and that we found no evidence for a fourth *DIFe* gene, there is no indication for the existence of *MT1*.

Plant *O*-methyltransferases constitute a large family with a wide spectrum of substrates (Lam et al., 2007), which were in most cases inferred by testing various compounds in *in vitro* assays or from sequence similarity to enzymes for which *in vitro* data are available. Our in vivo data show that such result should be interpreted with some caution. For example, the MT2 and MF enzymes exhibit high similarity to proteins annotated as CCoAMTs, but apparently cannot methylate these substrates. *Petunia* flowers only express activities that can methylate anthocyanins, but not cinnamic acids, and do not contain ferulic or sinapic acids (Jonsson et al., 1982). *In vitro* assays of methyltransferases often employ substrate concentrations in 0.1-1 mM range (e.g. Gang et al., 2002; Ibdah et al., 2003; Kim et al., 2006; Akita et al., 2011). Using similar anthocyanin substrate concentrations (0.4-1 mM), the AMTs in crude petal extracts, which originate from the three genes identified here, and recombinant MT2/DIFe1 protein could methylate anthocyanin 3-glucosides and 3-rutinosides *in vitro* (Jonsson et al., 1982) (Figure 2). *In vivo*, however, only little methylation of 3-rutinosides or their 3-glucoside precursors was seen, whereas efficient methylation occurred in petals synthesizing anthocyanin (3-acyl)rutinoside 5-glucosides, which matches well with the K_m values determined for AMTs in crude petals extracts (Jonsson et al., 1982). However, even when K_m or K_{cat}/K_m values for potential substrates are known, it remains difficult to ascertain the function in the absence of *in vivo* data, as (i) the *in vivo* concentrations of potential substrates (in the cytoplasm!) are difficult to

determine, (ii) the primary *in vivo* substrate(s) may have escaped attention in the *in vitro* assays, and (iii) enzymes competing for the same substrate are absent.

Gain and loss of functional AMT genes during evolution.

It is thought that the enzymes involved in anthocyanin synthesis evolved from enzymes in primary metabolism (Winkel-Shirley, 2001). The *DIFe* genes apparently originate from genes encoding methyltransferases involved in phenylpropapanoid metabolism, which required relatively small changes in the coding sequence to altered the substrate specificity of the encoded enzymes, and changes in *cis*-regulatory elements that brought them under the control of the MYB-HLH-WD40 complex that regulates many anthocyanin genes. Given that monocots, such as maize and rice do synthesize 3'and/or 5' methylated anthocyanins (Styles and Ceska, 1972; Yoshimura et al., 2012), but lack clear DIFe1/VvAOMT1 homologs, *AMT* genes may have evolved multiple times from different ancestors.

Subsequent modifications of AMT expression patterns as well as complete inactivation contributed to the diversification of anthocyanins *Petunia* species and varieties with functional methylation genes accumulate (3'5' methylated) malvidins in the petal limb and (3' methylated) petunidins in the tube. This seems largely due to the divergent expression patterns of *MT2*, which is about equally expressed in the petal limb and tube, and the *MF* genes, which are highly expressed in the limb and much less in the tube, indicating that tissue-specificity of decoration patterns can arise by alterations in *cis*-regulatory elements of some *AMT* genes.

P. axillaris accessions with limited (line S2) or no anthocyanin methylation (S1 and S26) contain *AMT* genes with disrupting mutations. This indicates that the last common ancestor of *P. axillaris* and *P. inflata* possessed functional *MF1, MF2* and *MT2* alleles and synthesized malvidins and that *P. axillaris* subsequently lost this capacity through loss of function mutations. Since the moth-pollinated *P. axillaris* flowers lack anthocyanins in the petal limb, where *MF* genes are mostly expressed, the inactivation of *MF1* and *MF2* might be due to the decreased selective pressure, after limb pigmentation was lost by inactivation of the MYB transcription factor AN2 (Quattrocchio et al., 1999; Hoballah et al., 2007). Because Arabidopsis lacks a clear MT/MF/VvAOMT1 homolog, the absence of methylated anthocyanins in this species (Saito et al., 2013) probably resulted from loss of function mutations as well.

Consequences of altered AMT substrate specificities: "the last will be first and the first will be last"

Other more subtle alterations in the coding sequences, which modified the substrate specificities of the AMTs, contributed to the diversification of the anthocyanins in at least two different ways. Distinct decorations of the anthocyanin could, in theory, take place in any order. Biochemical and genetic data indicate, however, that anthocyanin decoration is in *Petunia* a linear pathway rather than a grid in which different decorations are added in the strict order depicted in Figure 1A. The pathway that modifies anthocyanins in *Arabidopsis* is, although entirely different from the petunia pathway, also more linear than

grid-shaped (Saito et al., 2013). The strict order of modifications is established in two ways. Some enzymes add substituents that are subsequently modified by another enzyme. For example, RT has to add the rhamnose group before it can be acylated. Such directly interdependent reactions can only run in a fixed order that cannot be tinkered with during evolution. For other reactions their relative order is determined by the substrate-specificities of the enzymes and this is, in principle, more flexible. For example, in petunia acylation of the rhamnose group is required prior to 5-glucosylation and subsequent methylation because the 5GT does not accept anthocyanins without the acyl group as a substrate (Yamazaki et al., 2002) and MT2, MF1 and MF2 do not accept substrates without the acyl and/or 5-glucose moieties. This suggests that the substrate specificities of late enzymes, like MT2 and MF1/2, were adapted to that of enzymes catalyzing preceding steps, such as AAT and 5GT. It also envisages that alteration of the substrate specificity of AMTs to circumvent (or establish) the necessity for prior acylation or 5-glucosylation may produce a new repertoire of anthocyanins. The finding that VvAOMT1 can, unlike MT2 and MFs, methylate anthocyanin-rutinosides (or their 3-glucoside precursors), demonstrates that substrate specificities of homologous AMTs diverged indeed substantially, and explains why *Vitis* species and varieties synthesize simple 3-glucosides, or acetylated 3-glucosides of peonidin, petunidin and malvidin (Acevedo De la Cruz et al., 2012), while *Petunia* species or mutants cannot (Wiering, 1974; Ando et al., 1999).

Surprisingly, the malvidin 3-rutinosides and 3-glucosides found in petunia petals expressing VvAOMT1 are not acylated or 5-glycosylated. This suggests that the (precociously methylated) malvidins derivatives are not accepted by the petunia AAT or 5-GT enzyme as substrates. This implies that alterations in the specificity of one decorating enzyme, even the last enzyme of the pathway, may reshuffle the order in which decorations are added. Such a reshuffling of an entire part of a pathway provides new possibilities, but also constraints, by which evolutionary "tinkering" with substrate specificities of individual enzymes can create chemical diversity. Moreover, it suggests that the substrate specificities of distinct decorating enzymes are adjusted to one another in unforeseen ways, as late enzymes (in petunia: AMTs) are adapted to earlier enzymes (in petunia: AAT, 5GT) but also *vice versa*. Analysis of additional decorating enzymes, such as the AAT encoded by *GF* and homologs in other species may shed further light on this issue.

MATERIALS AND METHODS

Plant Material

Inbred *P. hybrida* lines were from the Amsterdam Petunia collection; relevant genotypes, as determined by Wiering and de Vlaming (unpublished data) in the 1970s and 1980s are given in Supplemental Table 4. Old Glory Blue is a commercial variety from Ball Seeds (Chicago, http://www.ballhort.com). Plant were grown and maintained throughout the year in a greenhouse with supplemental artificial lighting (cycles of 16hrs light and 8 hrs darkness) at a (minimum) temperature of 22 ^{o}C or higher. Tissues used for analysis of gene

expression and anthocyanin metabolites were harvested in the "summer period" (May-September), taking care that for direct comparisons tissues were harvested simultaneously.

Isolation and analysis of *DIFe* genes.

A cDNA library (1x 10^6 pfu) was constructed with a ZAP-cDNA Gigapack III Gold Cloning kit (Stratagene, http://www.genomics-agilent.com) using polyA$^+$ RNA isolated from petal tissue of *P. hybrida* cv Old Glory Blue and screened by hybridization with a *DIFe1* cDNA from V26. Genomic DNA sequences of *P. inflata* and *P. hybrida* were obtained using primers complementary to 5'UTR and 3'UTR sequences of the *DIFe1* and *DIFe2* cDNAs from OGB and V26. *P. axillaris* genomic sequences were obtained using primers (Supplemental Table 5) designed on (preliminary) genome sequence data provided by the petunia platform.

Enzymatic activity of DIFe1/MT2

For expression in *E. coli*, the *DIFe1* (*M2*) cDNA from OGB was amplified with the primers 1907*Bam*HI-FW (GCATGGATCCACAGGCAAAACCGCCCACCCTG) and 1907*Pst*I-RV (GCATCTGCAGCTAGGAGAG ACGCCTGCAAAG), digested with *Bam*HI and *Pst*I and ligated into the *E. coli* expression vector pQE30 (Qiagen) to yield pCGP3086. Cell free extracts were assayed for enzyme activity as described (Jonsson et al., 1983) using 0.5 mM delphinidin 3-glucoside, delphinidin 3-rutinoside, or delphinidin 3,5-diglucoside and S-adenosyl L methionine (SAM) as a methyl donor. Hydrolyzed reaction products (anthocyanidins) were analyzed by HPLC, and those obtained using ^{14}C-SAM by TLC and autoradiography, alongside standard samples of petunidin, malvidin and delphinidin.

Phylogenetic analysis

Sequence alignments were made with MUSCLE and phylogenetic trees with maximum-likelihood (PhyML) or neighbor-joining (BioNJ) and visualized with TreeDyn using web-based software (www.Phylogeny.fr) (Dereeper et al., 2008).

DNA and RNA gel-blot hybridization

DNA isolated from leaves (6 μg) was digested with EcoRI or BamHI, size-separated on a 0.9% agarose gel, blotted to nylon membranes by capillary transfer, hybridized at 42°C overnight in DIG Easy-Hyb buffer (Roche; http://www.roche-applied-science.com) using a digoxygenin-labeled *MF1* or *MT2* cDNA probe, washed under low stringency conditions (2xSSC, 25^{o}C), treated with high affinity anti-digoxigenin antibodies conjugated to alkaline phosphatase, incubated with the chemiluminescent substrate CSPD the membrane, and exposed to X-ray film. Subsequently the blot was rewashed at high stringency (0.1x SSC, 68^{o}C) and again exposed (1x SSC is 15mM Na_3-citrate, 150 mM NaCl). The same membrane was hybridized

twice, checking that any residual signal was completely eliminated from the membrane before the following hybridization. RNA gel-blot analysis was done as described previously (van Tunen et al., 1988).

Quantitative and Real-Time PCR

Real time PCR was performed using Power SYBER Green (Applied Biosystems; http://appliedbiosystems.com) using primers shown in Supplemental Table 6. Normalization was done based on the expression of *ACTIN*. Because *MF1* (*DIFe2a*) and *MF2* (*DIFe2b*) mRNAs were difficult to distinguish with primers suitable for Real-Time PCR, we used a previously described quantitative RT-PCR procedure (Souer et al., 2008) instead. This involved the amplification of specific mRNA products with gene-specific primers (Supplementary Table 7) using a reduced number of amplification cycles (20-25; depending on the abundance of the mRNA), to avoid reaching saturation and ensure a linear response, and detection of PCR products by DNA gel-blot hybridization with ^{32}P-labelled cDNA probes and Phosphorimaging, which ensures a quantitative detection of PCR products,

Transgenic plants

The coding sequence of *VvAOMT1* was amplified from berry cDNA using primers *VvOMT1*-F+attB1 and *VvOMT1*-R+attB2 and *MT2* from *P.hybrida M1* petal cDNA with primers *PhMT*-F+attB1 and *Ph*MT-R+attB2, recombined into the GATEWAY entry vector pDonor221 (Invitrogen), and subsequently recombined into destination vector pK2GW7.0 (Karimi et al., 2002). The *PhMF2* coding sequence was amplified from *P.hybrida* M1 petal cDNA with *PhMF*-F Topo primer and *PhMF*-R primer, cloned in pENTR/D Topo (Invitrogen, http://www.lifetechnologies.com) and subsequently recombined into pK2GW7.0. All constructs were introduced into *Agrobacterium tumefaciens* strain AGL0 by electroporation. A single colony was used for an overnight culture and used to infect petunia leaf discs. Primer sequences are shown in Supplemental Table 8.

Analysis of anthocyanins by LC-IT-TOF-MS-PDA

About 0.5 g fresh weight of petals were lyophilized and their anthocyanins extracted in 10 volumes 50 % acetonitrile containing 0.1 % trifluoroacetic acid. The extract was filtrated with PVDF membranes (0.45 µm, Merck Millipore, http://www.millipore.com) and 5 µl of the filtrate was injected to Inertsil ODS-4 column (4.6 mm X 250 mm, pore size 5 µm, GL-Sciences Inc., http://www.glsciences.com) for anthocyanin analysis using LCMS-IT-TOF (Shimadzu Corp., Kyoto) attached with photo diode array (Shimadzu Corp., http://www.shimadzu.com). The solvent system used included a linear gradient elution for 30 min from 90 % solvent A (0.1 % formic acid in H_2O) and 10 % solvent B (0.1 % formic acid and 90 % acetonitrile in H_2O) to 50 % solvent A and then for 15 min to 100 % solvent B. Different gradients were used occasionally. The flow rate was 0.6 min/min and the column temperature was 40 C. The absorption spectra were monitored

from 250 to 600 nm. MS and MS/MS were analyzed in *m/z* ranges of from 250 to 1,000 and from 100 to 1,000, respectively, in a positive mode after electrospray ionization.

Sequence data from this article can be found in the GenBank/EMBL databases under the following accession numbers: XXXXX (MT2), XXXXX (MF1), XXXXX (MF2).

Supplemental data

The following materials are available in the online version of this article

Supplemental Figure 1. Cladogram of plant O-methyltransferases

Supplemental Figure 2. Aligned sequences of wild type and mutant *MT2/DIFe1* alleles.

Supplemental Figure 3. Aligned sequences of wild type and mutant *MF1/DIFe2a* alleles.

Supplemental Figure 4. Aligned sequences of wild type and mutant *MF2/DIFe2a* a lleles.

Supplemental Figure 5. HPLC-PDA analysis of anthocyanidins and anthocyanins in petals expressing *35S:MT*, *35S:MF2* or *35S:VvAOMT1*.

Supplemental Figure 6. LC-MS/MS(+) analysis of anthocyanins in R78 petals and siblings expressing *35S:MT2*, *35S:MF2* or *35S:VvAOMT1*.

Supplemental Figure 7. LC-MS/MS (+) analysis of anthocyanins in R78xV32 petals.

Supplemental Figure 8. LC-MS/MS(+) analysis of anthocyanins in R78xV32 petals expressing *35S:MT2*

Supplemental Figure 9 LC-MS/MS(+) analysis of anthocyanins in R78xV32 petals expressing *35S:MF2*

Supplemental Figure 10. LC-MS/MS(-) analysis of peak 4 from R78xV32 petals expressing *35S:MF2*

Supplemental Figure 11. LC-MS/MS(+) analysis of anthocyanins in R78xV32 petals expressing *35S:VvAOMT1*.

Supplemental Figure 12. Structural models of *Ms* CCoA-MT in complex with anthocyanin substrates.

Supplemental Table 1. Methyltransferase activity in *E.coli* cells expressing DIFe1.

Supplemental Table 2. Genotypes of Petunia lines and derived F1 hybrids.

Supplemental Table 3. Primers used for amplification of *MT2*, *MF1* and *MF2* alleles.

Supplemental Table 4. Primer combinations used for quantitative RT-PCR.

Supplemental Table 5. Primers used for Real-Time PCR.

Supplemental Table 6. Primers used for construction of fusion genes.

Supplemental Table 7. Sequence alignment used for the phylogenetic tree in Figure S1 (Fasta format).

Supplemental Table 8. Sequence alignment used for the phylogenetic tree in Figure 4 (Fasta format)

ACKNOWLEDGEMENTS

We thank Pieter Hoogeveen, Martina Meesters and Daisy Kloos for plant care.

LITERATURE CITED

Acevedo De la Cruz A, Hilbert G, Riviere C, Mengin V, Ollat N, Bordenave L, Decroocq S, Delaunay JC, Delrot S, Merillon JM, Monti JP, Gomes E, Richard T (2012) Anthocyanin identification and composition of wild Vitis spp. accessions by using LC-MS and LC-NMR. Anal. Chim. Acta. **732:** 145-152

Akita Y, Kitamura S, Hase Y, Narumi I, Ishizaka H, Kondo E, Kameari N, Nakayama M, Tanikawa N, Morita Y, Tanaka A (2011) Isolation and characterization of the fragrant cyclamen O-methyltransferase involved in flower coloration. Planta **234:** 1127-1136

Alfenito MR, Souer E, Goodman CD, Buell R, Mol J, Koes R, Walbot V (1998) Functional complementation of anthocyanin sequestration in the vacuole by widely divergent glutathione *S*-transferases. Plant Cell **10:** 1135-1149

Ando T, Saito N, Tatsuzawa F, Kakefuda T, Yamakage K, Ohtani E, Koshi-ishi M, Matsusake Y, Kokubun H, Watanabe H, Tsukamoto T, Ueda Y, Hashimoto G, Marchesi E, Sakura K, Hara R, Seki H (1999) Floral anthocyanins in wild taxa of *Petunia* (Solanaceae). Biochem. Syst. Ecol. **27:** 623-650

Brouillard R, Chassaing S, Fougerousse A (2003) Why are grape/fresh wine anthocyanins so simple and why is it that red wine color lasts so long? Phytochemistry **64:** 1179-1186

Brugliera F, Holton TA, Stevenson TW, Farcy E, Lu CY, Cornish EC (1993) Isolation and characterization of a cDNA clone corresponding to the *Rt* locus of *Petunia hybrida*. Plant J. **5:** 81-92

Buer CS, Imin N, Djordjevic MA (2010) Flavonoids: new roles for old molecules. J. Integr. Plant Biol. **52:** 98-111

Comai L, Moran P, Maslyar D (1990) Novel and useful properties of a chimeric plant promoter combining CaMV 35S and MAS elements. Plant Mol Biol **15:** 373-381

de Vetten N, ter Horst J, van Schaik H-P, den Boer B, Mol J, Koes R (1999) A cytochome b5 is required for full acivity of flavonoid 3'5'-hydroxylase, a cytochrome P450 involved in the formation of blue flower colors. Proc. Natl. Acad. Sci. USA. **96:** 778-783

de Vlaming P, Cornu A, Farcy E, Gerats AGM, Maizonnier D, Wiering H, Wijsman HJW (1984) *Petunia hybrida*: A short description of the action of 91 genes, their origin and their map location. Plant Mol. Biol. Rep. **2:** 21-42

Dereeper A, Guignon V, Blanc G, Audic S, Buffet S, Chevenet F, Dufayard JF, Guindon S, Lefort V, Lescot M, Claverie JM, Gascuel O (2008) Phylogeny.fr: robust phylogenetic analysis for the non-specialist. Nucleic Acids Res **36:** W465-469

Ferrer JL, Zubieta C, Dixon RA, Noel JP (2005) Crystal structures of alfalfa caffeoyl coenzyme A 3-O-methyltransferase. Plant Physiol. **137:** 1009-1017

Gang DR, Lavid N, Zubieta C, Chen F, Beuerle T, Lewinsohn E, Noel JP, Pichersky E (2002) Characterization of phenylpropene O-methyltransferases from sweet basil: facile change of substrate specificity and convergent evolution within a plant O-methyltransferase family. Plant Cell **14:** 505-519

Grotewold E (2006) The genetics and biochemistry of floral pigments. Annu Rev Plant Biol **57:** 761-780

Hoballah ME, Gubitz T, Stuurman J, Broger L, Barone M, Mandel T, Dell'Olivo A, Arnold M, Kuhlemeier C (2007) Single gene-mediated shift in pollinator attraction in Petunia. Plant Cell **19:** 779-790

Hugueney P, Provenzano S, Verries C, Ferrandino A, Meudec E, Batelli G, Merdinoglu D, Cheynier V, Schubert A, Ageorges A (2009) A novel cation-dependent O-methyltransferase involved in anthocyanin methylation in grapevine. Plant Physiol. **150:** 2057-2070

Huits HSM, Gerats AGM, Kreike MM, Mol JNM, Koes RE (1994) Genetic control of dihydroflavanol 4-reductase gene expression in *Petunia hybrida*. Plant J. **6:** 295-310

Ibdah M, Zhang XH, Schmidt J, Vogt T (2003) A novel Mg(2+)-dependent O-methyltransferase in the phenylpropanoid metabolism of Mesembryanthemum crystallinum. J Biol Chem **278:** 43961-43972

Jonsson LMV, Aarsman MEG, de Vlaming P, Schram AW (1984) On the origin of anthocyanin methyltransferase isozymes of *Petunia hybrida* and their role in regulation of anthocyanin methylation. Theor. Appl. Genet. **68:** 459-466

Jonsson LMV, Aarsman MEG, Poulton JE, Schram AW (1984) Properties and genetic control of four methyltransferases involved in methylation of anthocyanins in flowers of *Petunia hybrida*. Planta **160:** 174

Jonsson LMV, Aarsman MEG, Schram AW, Bennink GJH (1982) Methylation of anthocyanins by cell-free extracts of flower buds of *Petunia hybrida*. Phytochemistry **21:** 2457-2459

Jonsson LMV, Aarsman MEG, Van Diepen J, Smit N, Schram AW (1984) Properties and genetic control of anthocyanidin 5-0-glucosyltransferase in flowers of *Petunia hybrida*. Planta **160:** 341-347

Jonsson LMV, de Vlaming P, Wiering H, Aarsman MEG, Schram AW (1983) Genetic control of anthocyanin-O-methyltransferase in flowers of *Petunia hybrida*. Theor. Appl. Genet. **66:** 349

Karimi M, Inze D, Depicker A (2002) GATEWAY vectors for Agrobacterium-mediated plant transformation. Trends Plant Sci. **7:** 193-195

Kim BG, Lee HJ, Park Y, Lim Y, Ahn JH (2006) Characterization of an *O*-methyltransferase from soybean. Plant Physiol Biochem **44:** 236-241

Koes R, Verweij CW, Quattrocchio F (2005) Flavonoids: a colorful model for the regulation and evolution of biochemical pathways. Trends Plant Sci. **5:** 236-242

Kroon J, Souer E, de Graaff A, Xue Y, Mol J, Koes R (1994) Cloning and structural analysis of the anthocyanin pigmentation locus *Rt* of *Petunia hybrida*: characterization of insertion sequences in two mutant alleles. Plant J. **5:** 69-80

Lam KC, Ibrahim RK, Behdad B, Dayanandan S (2007) Structure, function, and evolution of plant O-methyltransferases. Genome **50:** 1001-1013

Lucker J, Martens S, Lund ST (2011) Characterization of a Vitis vinifera cv. Cabernet Sauvignon 3',5'-O-methyltransferase showing strong preference for anthocyanins and glycosylated flavonols. Phytochemistry **71:** 1474-1484

Pichersky E, Gang DR (2000) Genetics and biochemistry of secondary metabolites in plants: an evolutionary perspective. Trends Plant Sci. **5:** 439-445

Provenzano S (2011) The genetics of anthocyanin production, accumulation and display: a comparative study in different species. PhD thesis. VU-University, Amsterdam

Quattrocchio F, Wing J, van der Woude K, Souer E, de Vetten N, Mol J, Koes R (1999) Molecular analysis of the *anthocyanin2* gene of *Petunia* and its role in the evolution of flower color. Plant Cell **11:** 1433-1444

Quattrocchio F, Wing JF, Leppen HTC, Mol JNM, Koes RE (1993) Regulatory genes controlling anthocyanin pigmentation are functionally conserved among plant species and have distinct sets of target genes. Plant Cell **5:** 1497-1512

Saito K, Yonekura-Sakakibara K, Nakabayashi R, Higashi Y, Yamazaki M, Tohge T, Fernie AR (2013) The flavonoid biosynthetic pathway in Arabidopsis: Structural and genetic diversity. Plant Physiol Biochem

Slimestad R, Aaberg A, Andersen OM (1999) Acylated anthocyanins from petunia flowers. Phytochemistry **50:** 1081-1086

Souer E, Rebocho AB, Bliek M, Kusters E, de Bruin RA, Koes R (2008) Patterning of inflorescences and flowers by the F-Box Protein DOUBLE TOP and the LEAFY Homolog ABERRANT LEAF AND FLOWER of *Petunia*. Plant Cell **20:** 2033-2048

Spelt C, Quattrocchio F, Mol J, Koes R (2000) *anthocyanin1* of petunia encodes a basic-Helix Loop Helix protein that directly activates structural anthocyanin genes. Plant Cell **12:** 1619-1631

Styles ED, Ceska (1972) Flavonoid pigments in genetic strains of maize Phytochemistry **11:** 3019-3021

van Houwelingen A, Souer E, Spelt C, Kloos D, Mol J, Koes R (1998) Analysis of flower pigmentation mutants generated by random transposon mutagenesis in *Petunia hybrida*. Plant J. **13:** 39-50

van Tunen AJ, Koes RE, Spelt CE, Van der Krol AR, Stuitje AR, Mol JNM (1988) Cloning of the two chalcone flavanone isomerase genes from *Petunia hybrida*: Coordinate, light-regulated and differential expression of flavonoid genes. EMBO J. **7:** 1257-1263

Wang J, Pichersky E (1999) Identification of specific residues involved in substrate discrimination in two plant O-methyltransferases. Arch Biochem Biophys **368:** 172-180

Wiering H (1974) Genetics of flower colour in *Petunia hybrida* Hort. Genen Phaenen **17:** 117-134

Wiering H, De Vlaming P (1977) Glycosylation and methylation patterns of anthocyanins in *Petunia hybrida*. II. The genes *Mf1* and *Mf2*. Z. Pfanzenzüchtung **78:** 113-123

Winkel-Shirley B (2001) Flavonoid biosynthesis. A colorful model for genetics, biochemistry, cell biology, and biotechnology. Plant Physiol. **126:** 485-493

Yamazaki M, Yamagishi E, Gong Z, Fukuchi-Mizutani M, Fukui Y, Tanaka Y, Kusumi T, Yamaguchi M, Saito K (2002) Two flavonoid glucosyltransferases from *Petunia hybrida*: molecular cloning, biochemical properties and developmentally regulated expression. Plant Mol. Biol. **48:** 401-411.

Yoshimura Y, Zaima N, Moriyama T, Kawamura Y (2012) Different localization patterns of anthocyanin species in the pericarp of black rice revealed by imaging mass spectrometry. PLoS One **7:** e31285

Zubieta C, He XZ, Dixon RA, Noel JP (2001) Structures of two natural product methyltransferases reveal the basis for substrate specificity in plant O-methyltransferases. Nat Struct Biol **8:** 271-279

Zubieta C, Ross JR, Koscheski P, Yang Y, Pichersky E, Noel JP (2003) Structural basis for substrate recognition in the salicylic acid carboxyl methyltransferase family. Plant Cell **15:** 1704-1716

Legends

Figure 1. Role of loci and enzymes required for methylation of anthocyanins.

A, Diagram depicting the modification of simple anthocyanin 3-glucosides by subsequent rhamnosylation, 5-glucosylation, acylation and methylation. Enzymes involved in each reaction are indicated on the right of the arrows and genetic loci (italics) controlling the reaction on the left. B, RNA gel blot analysis of *DIFe1* expression in petals of four inbred petunia lines that are homozygous for functional (+) or mutant alleles (-) of *MT2*, *MF1* and *MF2*. Abbreviations: 5GT, Anthocyanin 5-glucosyltransferase,: AAT, Anthocyanin acyltransferase,: A3'MT, Anthocyanin 3'-methyltransferase; A3'5'MT, Anthocyanin 3'5'-methyltransferase; *RT*, *RHAMNOSYLATION AT THREE*; *GF*, *GLUCOSYLATION AT FIVE*; *MT*, *METHYLATION AT THREE*; *MF*, *METHYLATION AT FIVE*.

Figure 2. Methylation of anthocyanins by *DIFe1* and *DIFe2 in vitro* and *in vivo*.

(A) Anthocyanidins (% of total) after incubation of SAM and the 3-glucoside (3G), 3-rutinoside (3R) or 3,5 diglucoside (3,5G) of delphinidin with crude extracts of *E.coli* expressing DIFe1, the empty vector or no extract at all (none). Mal, malvidin; Pet, petunidin; Del, delphinidin; Peo, peonidin; Cya, cyanidin.

(B) Phenotype of a flower from a control plant and *MAC:asDIFe1* transformant #A.

(C) Composition of anthocyanidins in flowers of distinct *MAC:asDIFe1* and *MAC:asDIFe2* lines and a control plant without transgene.

Figure 3. DNA gel-blot analysis of *DIFe* genes/paralogs in *P. hybrida*.

DNA from *P. hybrida* lines M1, V30 and R78 was digested with EcoRI (E) or BamHI (B), size separated, hybridized to $DIFe2^{OGB}$ cDNA, washed at low stringency (2x SSC, 25°C; left panel), and subsequently at high stringency (0.1x SSC 68°C: middle panel), or hybridized with the *DIFe1* cDNA and washed using high stringency conditions (right panel). Fragments hybridizing to *DIFe1* and *DIFe2* at high stringency are marked with white and black arrowheads respectively.

Figure 4. Phylogram of A1-type plant O-methyltransferases.

The tree (maximum likelihood) is based on a cured sequenced alignment (Supplemental Table 3). Numbers on branches indicate percent bootstrap support (500 replicates). For each protein the name, accession number, and substrates accepted *in vitro* is given. Prefixes indicate the species of origin: *At*, *Arabidopsis thaliana*; *Ckm, Cyclamen persicum x purpurascens*; *Fv, Fragaria vesca*; *Mc, Mesembryanthemum crystallinum*; *Ms, Medicago sativa*; *Nt, Nicotiana tabacum*; *Os, Oryza sativa*; *Pc, Petroselinum crispum*; *Ph, Petunia hybrida*; *Pp, Prunus persica*; *Pt, Populus trichocarpa*; *Sl, Solanum lycopersicum*; *St, Solanum tuberosum*; *Stl, Stellaria longipes*; *Vv Vitis vinifera*; *Zm, Zea mays*; *Zv, Zinnia violacea*.

Figure 5. Expression pattern and regulation of *DIFe* genes.

A, Quantitative RT-PCR analysis of *MT2*, *MF1* and *MF2* mRNAs in different tissues of the *P. hybrida* F1 hybrid M1xV30. Floral tissues were from buds of three different stages. Stage 1/2, buds up to 20 mm; stage 3-4, bud 30-40 mm; stage 5-6, open flowers. *GAPDH* and *ACTIN* were used as internal controls. B, Real time-PCR analysis of mRNAs expressed in stage 3-4 petals of regulatory mutants. Lines R27 (*AN1 AN2 AN11*), W225 (*an1*) and W134 (*an11*) are isogenic. Line W242 is in a distinct genetic background and harbors a mutable *an2* allele ($an2^{mut}$). A germinal $AN2^{REV}$ revertant in which the transposon had excised from *AN2* was used as an isogenic wild type. mRNA levels were normalized using *ACTIN* and expression in R27 was set to 1. Primers used for Real-time PCR could not distinguish between *DIFe2a*/*MF1* and *DIFe2b*/*MF2*.

Figure 6. Structure of wild type and mutant alleles of *MT2* (*DIFe1*), *MF1* (*DIFe2b*) and *MF2* (*DIFe2a*).

A, Quantitative RT-PCR analysis of *DIFe* mRNAs in genotypes with *mt*, *mf1* and/or *mf2* alleles.

B, Structure of *DIFe1*/*MT2* locus in *P. hybrida* (*Ph*), *P. inflata* (*Pi*) and *P. axillaris* (*Pa*) lines with different *MT2 MF1 MF1* genotypes. (+, homozygous for dominant allele; - homozygous for recessive non-functional allele, x homozygous dominant for *MF1* and/or *MF2*). C, Structure of *DIFe2a*/*MF1* and *DIFe2b*/*MF2* locus in *P. hybrida* (*Ph*), *P. inflata* (*Pi*) and *P. axillaris* (*Pa*) lines with different genotypes. Coding and non-coding sequences (introns are not drawn to scale) are indicated by rectangles and lines, respectively, and start and stop codons by open and closed circles. Numbers denote the number of nucleotides in (functional) exons, and introns. Lesions found in mutant alleles are indicated above the gene maps.

Figure 7. Complementation of *mf* and *mt* mutants by *35S:MT2*, *35S:MF2 and* 35S:*VvAOMT1*.

A, Flowers of an untransformed R78 and R78xV32 plants and transgenic siblings that express *35S:MT2*, *35S:MF2* or *35S:VvAOMT1*. Hashtags indicate specific transformants. B, Composition of anthocyanidins obtained by acid hydrolysis of anthocyanins in petals of transgenic and control plants, as determined by HPLC. C, LC-MS/MS analysis of anthocyanins in R78 petals (control) and transgenic siblings expressing *35S:MT2, 35S:MF2* or *35S:VvAOMT1*.. D, Quantitative RT-PCR analysis of transgene expression in distinct transformants. Hashtags (#) denote individual transformants. E, LC-MS/MS analysis of anthocyanins in R78xV32 petals (control) and transgenic siblings expressing *35S:MT2, 35S:MF2* or *35S:VvAOMT1*.

Diagrams in (C) and (E) show LC profiles and for the major peaks *m/z* values of the corresponding ion and, in brackets, subfragments observed in MS/MS(+) spectra (see Supplemental Figures 4-9).

Figure 8. Two possible binding modes of delphinidin 3-(coumaroyl) rutinoside 5-glucoside.

A, Alignment of CCoAMTs and AMTs. Amino acids and motifs of *Ms* CCoAMT involved in dimerization, binding of SAM/SAH (*S*-adenosyl-L-homocysteine), the caffeoyl or CoA moiety, and divalent cation are indicated. B, Substrate binding with the 3-(coumaroyl)rutinoside chain pointing into the active site and clashing with bulky residues (Tyr208, Tyr212), which are in the petunia AMTs replaced by smaller ones (Gly, Leu). For clarity the 5-glucose group of the anthocyanin is not shown. C, Side view of B. D, Substrate binding with the 3-(coumaroyl)rutinoside chain oriented towards the active site and clashing with bulky residues (Trp58, Asn116, Tyr 208) which are in the petunia AMTs replaced by Ala/Gly, Ala and Gly respectively. For clarity the 5-glucose group of the anthocyanin is not shown. E, Side view of D.

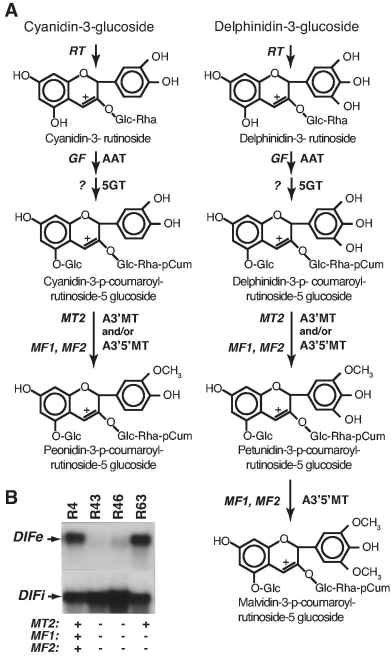

Figure 1. Role of loci and enzymes required for methylation of anthocyanins.

A, Diagram depicting the modification of simple anthocyanin 3-glucosides by subsequent rhamnosylation, 5-glucosylation, acylation and methylation. Enzymes involved in each reaction are indicated on the right of the arrows and genetic loci (italics) controlling the reaction on the left.

B, RNA gel blot analysis of *DIFe1* expression in petals of four inbred petunia lines that are homozygous for functional (+) or mutant alleles (-) of MT2, MF1 and MF2.

Abbreviations: 5GT, Anthocyanin 5-glucosyltransferase,: AAT, Anthocyanin acyltransferase,: A3'MT, Anthocyanin 3'-methyltransferase; A3'5'MT, Anthocyanin 3'5'-methyltransferase; RT, RHAMNOSYLATION AT THREE; GF, GLUCOSYL-ATION AT FIVE; MT, METHYLATION AT THREE; MF, METHYLATION AT FIVE.

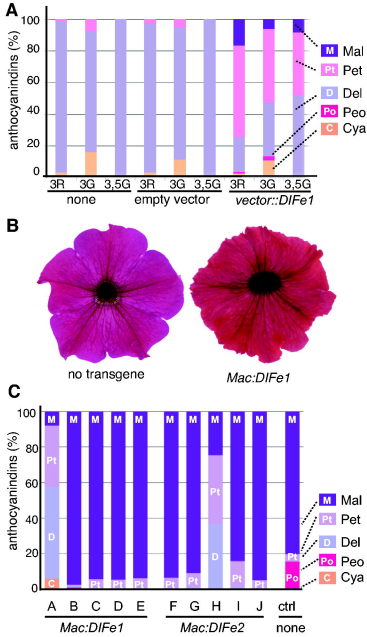
(%)
100
80
60
40
20
0
3R
3G
3,5G
none
empty vector
vector::DIFe1
M Mal
Pt Pet
D Del
Po Peo
C Cya
B
no transgene
Mac:DIFe1
C
A B C D E
F G H I J
ctrl
none
Mac:DIFe1
Mac:DIFe2

Figure 2. Methylation of anthocyanins by *DIFe1* and *DIFe2 in vitro* and *in vivo*.

A, Anthocyanidins (% of total) after incubation of SAM and the 3-glucoside (3G), 3-rutinoside (3R) or 3,5 diglucoside (3,5G) of delphinidin with crude extracts of *E.coli* expressing DIFe1, the empty vector or no extract at all (none). Mal, malvidin; Pet, petunidin; Del, delphinidin; Peo, peonodin; Cya, cyanidin.

B, Phenotype of a flower from a control plant and *MAC:asDIFe1* transformant #A.

C, Composition of anthocyanidins in flowers of distinct *MAC:asDIFe1* and *MAC:asDIFe2* lines and a control plant without transgene.

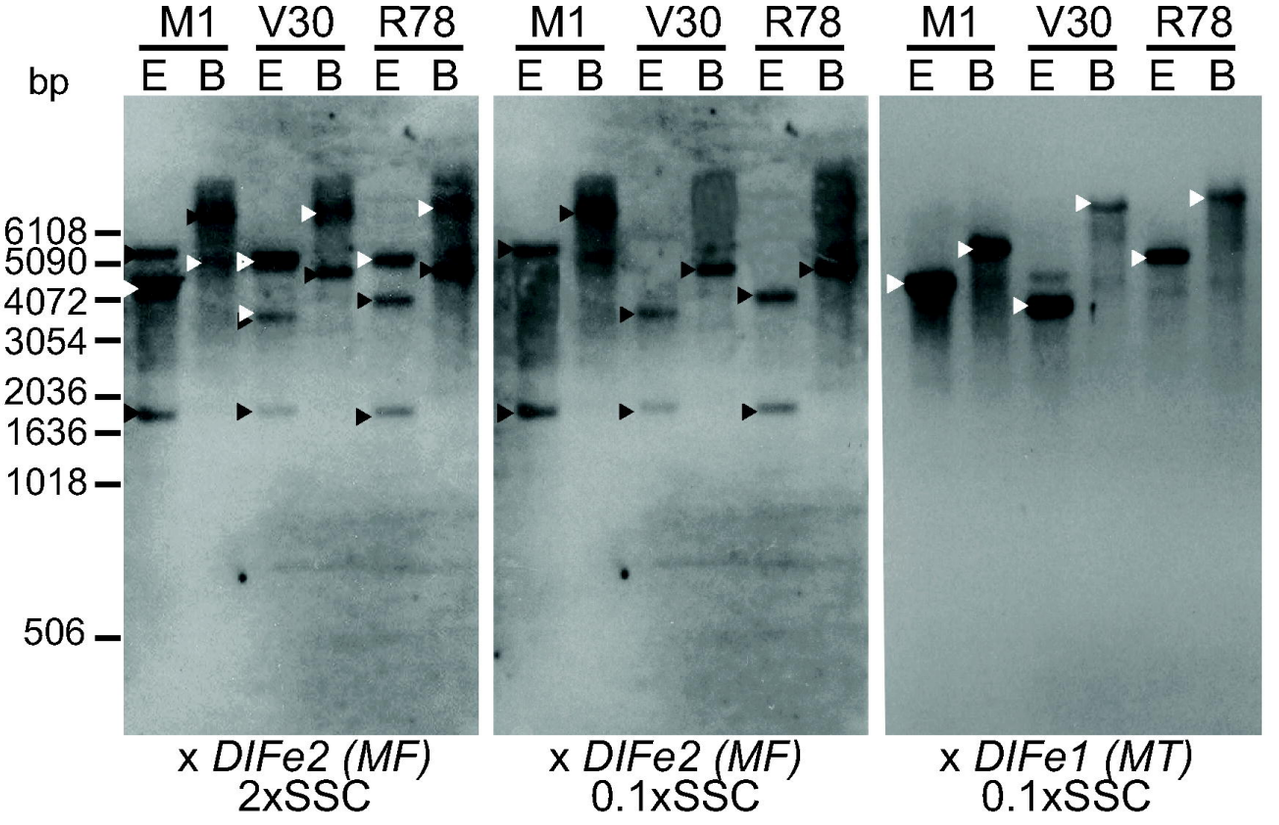

Figure 4. DNA gel-blot analysis of DIFe genes/paralogs in P. hybrida. DNA from *P. hybrida* lines M1, V30 and R78 was digested with EcoRI (E) or BamHI (B), size separated and hybridized to *DIFe2*^{OGB} cDNA washed at low stringency (2x SSC, 25°C; left panel), and subsequently (re)washed at high stringency (0.1x SSC 68°C: middle panel), or hybridized with the *DIFe1* cDNA and washed at high stringency (right panel). Fragments hybridizing to *DIFe1* and *DIFe2* at high stringency are marked with white and black arrowheads respectively.

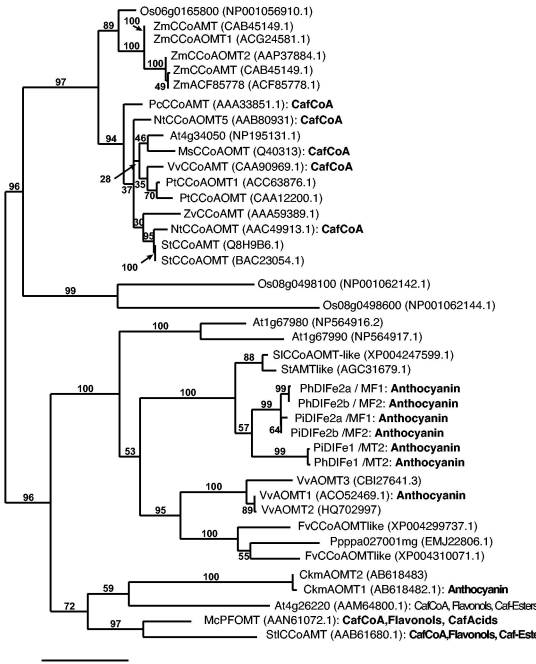

Figure 3. Phylogram of A1-type plant O-methyltransferases belonging
The tree (maximum likelihood) is based on a cured sequenced alignment. Numbers on branches indicate bootstrap support (500 replicates). For each protein the name, accession number, and substrates accepted *in vitro* is given. Prefixes indicate the species of origin: *At, Arabidopsis thaliana; Ckm, Cyclamen persicum x purpurascens; Fv, Fragraria vesca; Mc Mesembryanthemum crystallinum; Ms, Medicago sativa; Nt, Nicotiana tabacum; Os, Oryza sativa; Pc, Petroselinum crispum; Ph, Petunia hybrida; Pp, Prunus persica; Pt, Populus trichocarpa; Sl, Solanum lycopersicum; St, Solanum tuberosum; Stl, Stellaria longipes; Vv Vitis vinifera; Zm, Zea mays; Zv, Zinnia violacea.*

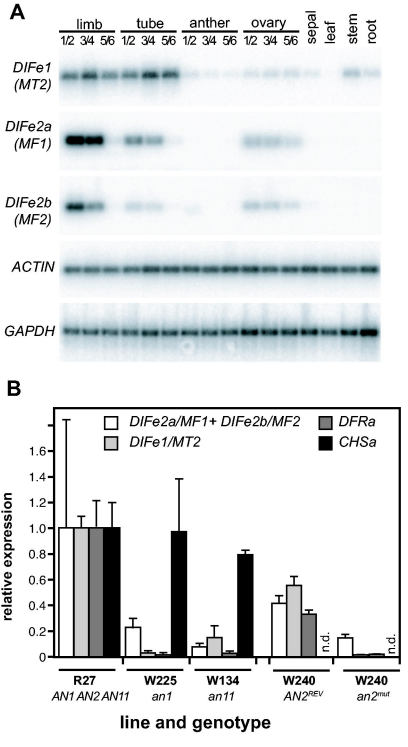

Figure 5. Expression pattern and regulation of DIFe genes.
(A) Quantitative RT-PCR analysis of *MT2, MF1 and MF2* mRNAs in different tissues of the *P. hybrida* F1 hybrid M1xV30. Floral tissues were from buds of three different stages. Stage 1/2, buds up to 20 mm; stage 3-4, bud 30-40 mm; stage 5-6, open flowers. *GAPDH* and *ACTIN* were used as internal controls.
(B) Real time-PCR analysis of mRNAs expressed in stage 3-4 petals of regulatory mutants. Lines R27 (*AN1 AN2 AN11*), W225 (*an1*) and W134 (*an11*) are isogenic. Line W242 is in a distinct genetic background and harbors a mutable *an2* allele (an2mut). A germinal $AN2^{REV}$ revertant in which the transposon had excised from *AN2* was used as an isogenic wild type. mRNA levels were normalized using *ACTIN* and expression in R27 was set to 1. Primers used for Real-time PCR could not distinguish between *DIFe2a/MF1* and *DIFe2b/MF2*.

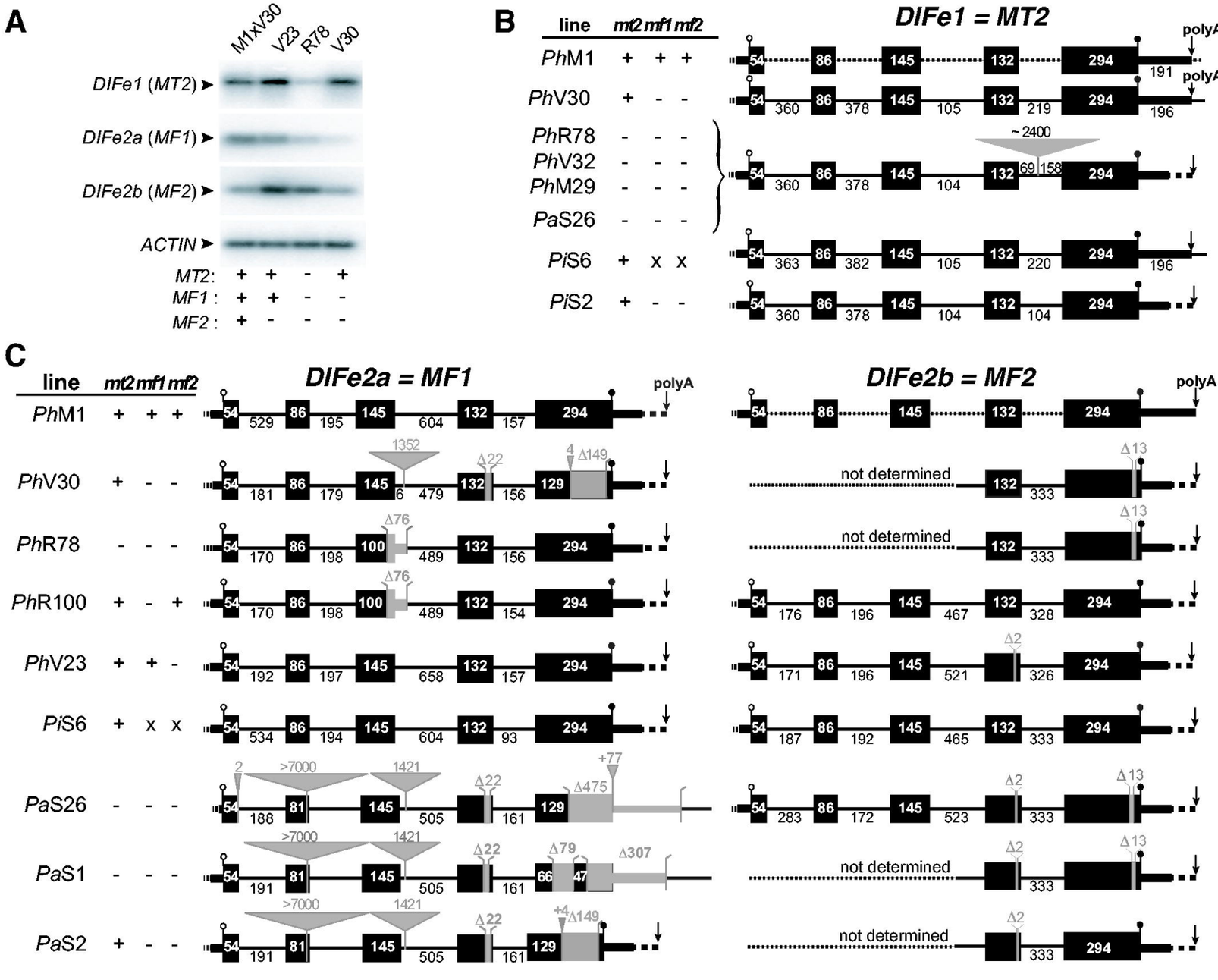

Figure 6. Structure of wild type and mutant alleles of *MT2* (*DIFe1*), *MF1* (*DIFe2b*) and *MF2* (*DIFe2a*).

A, Quantitative RT-PCR analysis of *DIFe* mRNAs in genotypes with *mt2, mf1* and/or *mf2* alleles.

B, Structure of *DIFe1/MT2* locus in *P. hybrida* (*Ph*), P. inflata (*Pi*) and *P. axillaris* (*Pa*) lines with different *MT2 MF1 MF1* genotypes. (+, homozygous for dominant allele; - homozygous for recessive non-functional allele, x homozygous dominant for *MF1* and/or *MF2*)

C, Structure of *DIFe2a/MF1* and *DIFe2b/MF2* locus in *P. hybrida* (*Ph*), *P. inflata* (*Pi*) and *P. axillaris* (*Pa*) lines with different genotypes.

Coding and non-coding sequences (introns are not drawn to scale) are indicated by rectangles and lines, respectively, and start and stop codons by open and closed circles. Numbers denote the number of nucleotides in (functional) exons, and introns. Lesions found in mutant alleles are indicated above the gene maps.

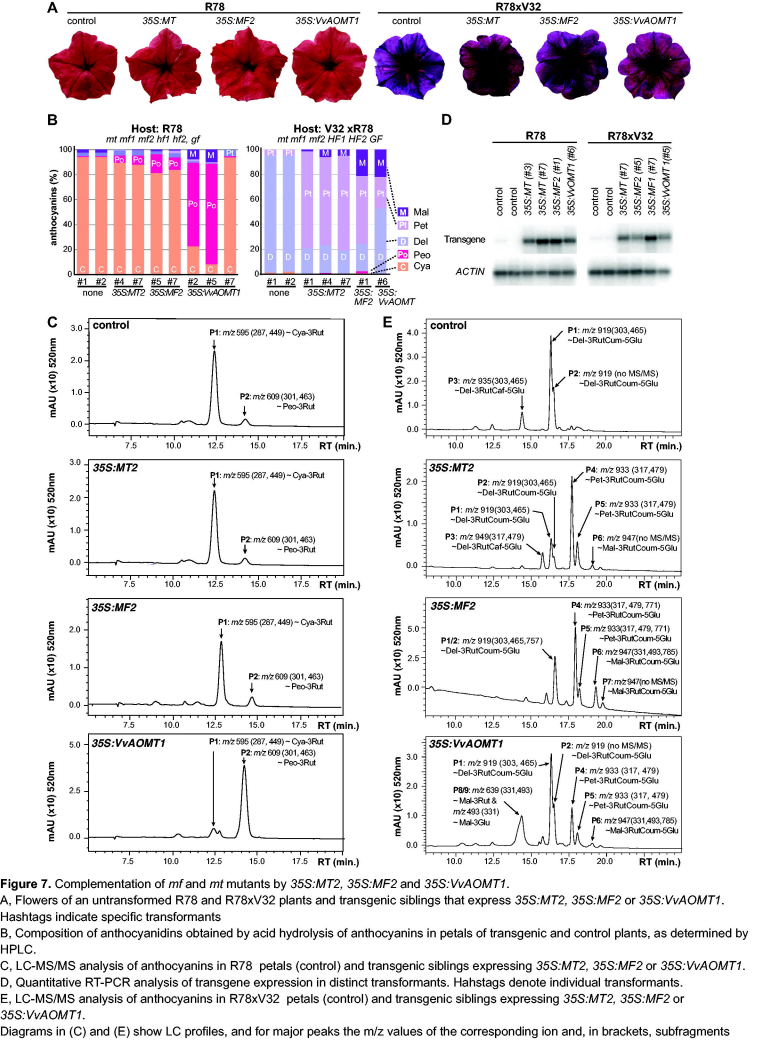

Figure 7. Complementation of *mf* and *mt* mutants by *35S:MT2, 35S:MF2* and *35S:VvAOMT1*.

A, Flowers of an untransformed R78 and R78xV32 plants and transgenic siblings that express *35S:MT2, 35S:MF2* or *35S:VvAOMT1*. Hashtags indicate specific transformants

B, Composition of anthocyanidins obtained by acid hydrolysis of anthocyanins in petals of transgenic and control plants, as determined by HPLC.

C, LC-MS/MS analysis of anthocyanins in R78 petals (control) and transgenic siblings expressing *35S:MT2, 35S:MF2* or *35S:VvAOMT1*.

D, Quantitative RT-PCR analysis of transgene expression in distinct transformants. Hahstags denote individual transformants.

E, LC-MS/MS analysis of anthocyanins in R78xV32 petals (control) and transgenic siblings expressing *35S:MT2, 35S:MF2* or *35S:VvAOMT1*.

Diagrams in (C) and (E) show LC profiles, and for major peaks the m/z values of the corresponding ion and, in brackets, subfragments observed in MS/MS(+) spectra shown in Supplemental Figures 4-9 online.

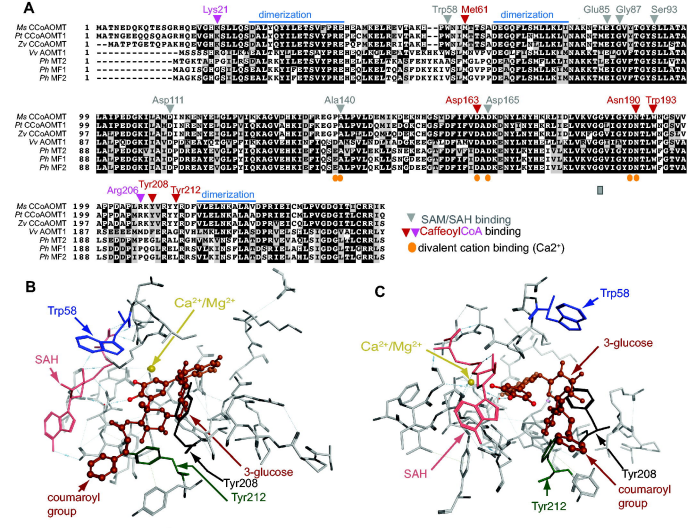

Figure 8. Two possible binding modes of delphinidin 3-(coumaroyl) rutinoside 5-glucoside.

A, Alignment of CCoAMTs and AMTs. Amino acids and motifs of *Ms* CCoAMT involved in dimerization, binding of SAM, the caffeoyl or CoA moiety, and divalent cation are indicated.

B, Substrate binding with the 3-(coumaroyl)rutinoside chain pointing into the active site and clashing with bulky residues (Tyr208, Tyr212), which are in the petunia AMTs replaced by smaller ones (Gly, Leu). For clarity the 5-glucose group of the anthocyanin is not shown.

C, Side view of B.

D, Substrate binding with the 3-(coumaroyl)rutinoside chain oriented towards the active site and clashing with bulky residues (Trp58, Asn116, Tyr 208) which are in the petunia AMTs replaced by Ala/Gly, Ala and Gly respectively. For clarity the 5-glucose group of the anthocyanin is not shown.

E, Side view of D.